

Approximate Quantum Algorithms as a Multiphoton Raman Excitation of a Quasicontinuum Edge

A. Mandilara,¹ Daniil Fedotov,² and V. M. Akulin^{3,4}

¹*Department of Informatics and Telecommunications,
National and Kapodistrian University of Athens, Panepistimiopolis, Ilisia, 15784, Greece*

²*Department of Electrical Engineering, Higher School of Economics,
34, Tallinskaya st., Moscow, 123458, Russia.(on leave)*

³*Laboratoire Aimé-Cotton CNRS UMR 9025, L'Université Paris-Saclay,*

Bât. 505, Campus d'Orsay, Rue Aimé-Cotton, 91405 Orsay Cedex, France.

⁴*Institute for Information Transmission Problems of the Russian Academy of Science,
Bolshoy Karetny per. 19, Moscow, 127994, Russia.(on leave)*

Many quantum algorithms can be seen as a transition from a well-defined initial quantum state of a complex quantum system, to an unknown target quantum state, corresponding to a certain eigenvalue either of the Hamiltonian or of a transition operator. Often such a target state corresponds to the minimum energy of a band of states. In this context, approximate quantum calculations imply transition not to the single, minimum energy, state but to a group of states close to the minimum. We consider dynamics and the result of two possible realization of such a process – transition of population from a single initially populated isolated level to the quantum states at the edge of a band of levels. The first case deals with the time-independent Hamiltonian, while the other with a moving isolated level. We demonstrate that the energy width of the population energy distribution over the band is mainly dictated by the time-energy uncertainty principle, although the specific shape of the distribution depends on the particular setting. We consider the role of the statistics of the coupling matrix elements between the isolated level and the band levels. We have chosen the multiphoton Raman absorption by an ensemble of Rydberg atoms as the model for our analysis, although the results obtained can equally be applied to other quantum computing platforms.

I. THE CONTEXT OF THE PROBLEM

Interaction of an isolated level with a large number of other states is the well-known classical problem that is often encountered in different domains of Quantum Physics and Physical Chemistry. Active research in the field of Quantum Computing during the last decade brought to the fore an important facet of this problem – how to efficiently populate states of a continuous spectrum edge. In this paper we consider a number of possible regimes of the population dynamics taking place at a quasi-continuum edge in the course of its interaction-induced excitation.

The problem of a level interacting with a band has a very long history, which starts from the Fermi's golden rule and has its continuation in many other publications revealing various aspects of the process, such as the population distribution over the energy scale considered by Jortner and Bixon [2], the interference induced by the presence of a strong coupled level known as Fano profile [3], the role of the level motion considered by Demkov and Osherov [4], and the role of the level couplings statistics [5], among other papers in this field. All these aspects are also important at the spectrum edge, affecting the rate at which the transition occurs and the energy width of the population distribution.

A first indication of the underlying relation between level-band problems and quantum computing was given with the introduction of the adiabatic quantum computation model [6]. In this model the solution to a classical problem is mapped into the ground state of the spec-

trum of a many-body Hamiltonian and the role of the quantum algorithm is to prescribe the adiabatic procedure for reaching the latter. Soon it became evident that for the most interesting combinatorial problems [7] the required, for the success of the adiabatic procedure, gap between the ground state and the rest of the spectrum, is not guaranteed. As a result new algorithmic procedures [8] appeared with the aim to offer approximate solutions to such optimization problems and which can potentially give results even in the absence of a gap. These approximate methods having also the advantage of requiring less physical resources, have attracted the interest of the community during the last years. In short, the generic prescription for reaching the edge of the spectrum is to adjust the parameters, such as application times of fixed control signals, in accordance with classically processed feedback from the quantum system. The results of the current work, also provide guidance for populating quantum states at the edge of the spectrum although the procedure under consideration is designed for a specific quantum ‘hardware’, i.e., arrays of Rydberg atoms, exploiting long-standing theoretical and experimental knowledge on such physical systems. Recent experiments [15] demonstrate the actuality of such a choice.

It is worth mentioning that the straightforward dipole-dipole mechanism is not the only possible way to create interaction among atoms. A more general case of interaction can be constructed by periodic change of the positions of interacting atoms, which can be seen as periodic sequence of unitary operations applied to single atoms, pairs of them, and to groups of a few atoms. Quantum

evolution in this case can be interpreted as action of an "effective" Hamiltonian given by the logarithm of the unitary transformation over the period. In the presence of an external electromagnetic field, one can therefore speak about the controlled multi-quantum transitions among the eigenstates of this Hamiltonian, the quasienergy levels of the atomic ensemble under periodic manipulations. The aim remains the same – to populate the lowest level of the quasienergy band, if we speak about the exact algorithm, or to transfer population to a narrow strip of the levels nearest to the edge, when admitting approximate algorithms. Coherence time for such a setting is dictated by the accuracy with which the periodic operations are performed.

The paper is organized as follows. We start by presenting a well-known physical model of quantum computation based on an ensemble of Rydberg atoms interacting with an electromagnetic field in the regime of the dipole-dipole blockade [10] and discuss how it can be seen in terms of the multiphoton transitions. We then remind the main features of the level-band system dynamics employing qualitative images that help to better perceive different excitation regimes. After these introductory sections, we turn to the main part of the paper by considering the excitation of a uniform continuum edge after an abrupt switch-on interaction, and calculate the energy distribution of the population and the required time it to attain. At a further step, we discuss the possibility of narrowing the distribution by slowly approaching the level from the infinitely far energy position to the edge and back and discuss the regime where the distribution width is limited just by the frequency-time uncertainty principle. Next question we address is the role of the distribution of the coupling energies between the level and the states of the continuum. We show that the continuum inhomogeneity is capable of "spoiling" the energy distribution under certain conditions. We conclude by considering a rather general case of the coupling statistics and identify the regime where a rather narrow population distribution at the continuum edge can be achieved in spite of the presence of the "spoiling states". We finally discuss what the obtained results mean for the approximate quantum algorithms.

II. THE MODEL

There are many possible physical realization of two-level models suitable for Quantum Calculations. We focus on one of them – an ensemble of two-level Rydberg atoms, where both of levels correspond to the highly excited Rydberg states coupled to the external intensive and highly coherent RF field by dipole interaction. The RF field itself can be either monochromatic, such that the field frequency is close to the frequency of the transition between the Rydberg states, or contain more harmonics, such that the transition frequency and the field frequencies are close to the condition of a multiphoton

Raman resonance. The long wavelength of the RF radiation implies that all the ensemble atoms are placed in the same external field. At the same time, periodic manipulations exert upon the atomic position by the technique of optical tweezers allows one to realize the effective multiparticle interactions among atoms in addition to their regular second-order van der Waals dipole interactions. The lower Rydberg state will hereafter be referred as the ground state, while the upper Rydberg state as "excited".

There are also many possible formulation of the mathematical problem which is supposed to be solved by physical realization of a Quantum Algorithm. The most known formulation requires population of the lowest energy eigenstate, or at least the eigenstates close in energy to the minimum. Here we focus on a slightly different formulation of the problem and require population of the state corresponding to the minimum energy per excited atom. The multiphoton Raman excitation enable one to select from the entire variety of such states some sub-manifolds satisfying the Raman resonance condition. In a sense, it is a more general formulation of the mathematical problem, which however is equivalent to the most known problem from the point of view of the complexity theory.

In order to be more specific, let us consider the Hamiltonian of such an ensemble of N two-level atoms without RF field in the form

$$\hat{H} = \sum_{n=1}^N \hbar\omega\hat{\sigma}_{z,n} + F(\{\hat{\sigma}_{z,n}\}), \quad (1)$$

which consist of the sum of individual atomic Hamiltonian $\hbar\omega\hat{\sigma}_{z,n}$ and a nonlinear function $F(\{\hat{\sigma}_{z,n}\})$ given in terms of the Pauli operators $\hbar\omega\hat{\sigma}_{z,n}$. The nonlinear function is constructed with the help of the second order van der Waals coupling and the periodic control technique in such a way, that it takes the minimum value per excited atom for a quantum state of the ensemble corresponding to the solution of a mathematical problem of interest.

The Hamiltonian Eq.(1) is diagonal in the basis of direct products of the lower and upper states of the atoms. This is the so-called "computational" basis, where each of its eigenstate has the form

$$|0, 1, \dots, 1, 0\rangle$$

and corresponds to the binary representation of an integer, encoded in the distribution of the excitation of different atoms whence each atom corresponds to a certain register of this binary encoding. Position of the lowest eigenvalue is supposed to be known. What is required is to find the eigenvector corresponding to this lowest eigenvalue in the computational basis. Our aim is therefore to transfer all the population from the ground state of the atomic ensemble to this very state, or at least, to a group of states close to the minimum energy per atom. Once this goal achieved, by measuring the excitations distribution among individual atoms, one finds the required integer – either the exact solution of the mathematical

problem encoded in the Hamiltonian \hat{H} via the nonlinear function $F(\{\hat{\sigma}_{z,n}\})$, or an approximate solution – another number, which gives the energy value close to the minimum.

The Hamiltonians are realized by constructing the interatomic interactions. One may think of finding the minimum energy for the Ising problem, as an example. A more general example of the spectrum of an ensemble of seven atoms generated by a random choice of constants of the binary, triple, and four-body interatomic interactions is depicted in Fig.1.

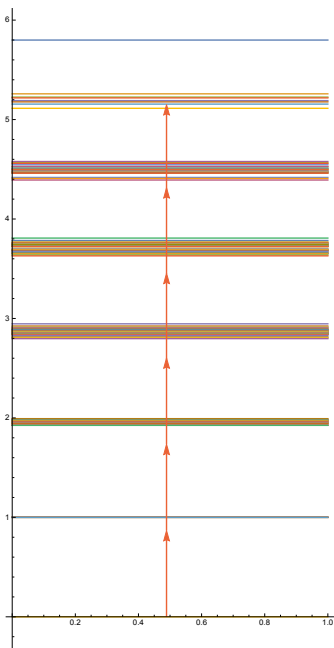


FIG. 1: The energy spectrum E_s of seven two-level atoms interacting via their $\hat{\sigma}_z$. Parameter of two, three, and four-particle interactions are chosen randomly. This spectrum mimics a spectrum of Hamiltonian constructed for finding a minimum energy per atom for a specific problem. By arrows we depict energies corresponding to the absorption of a number of photons. For the chosen parameters, the minimum energy per atoms corresponds to the excitation of six atoms.

As a possible physical realization of such an ensemble, one may think of a number of two-level Rydberg atoms placed in a certain fixed positions in the space in the presence of the magnetic field along z axis. Then the second order dipole-dipole perturbation will introduce the binary coupling

$$\sum_{n < m} C \frac{\hat{\sigma}_{z,n} \hat{\sigma}_{z,m}}{R_{mn}^6},$$

known as dipole blockade, where R_{mn} stands for the distance between every pair of atoms, and C is a constant accounting for the atomic dipole susceptibility. The higher order interactions, say the three-body and the four-body ones, in principle can also be induced, though

with much more involved procedures relying on the multiphoton processes based on virtual transitions to the neighboring Rydberg states, different from the two levels under consideration, that would favor the higher-order nonlinear susceptibilities. This process may equally include addressing and manipulation of the position of individual atoms by implementing optical tweezers. These actions can be seen here as construction of the effective interatomic interaction Hamiltonian $F(\{\hat{\sigma}_{z,n}\})$ of Eq.(1).

In an external RF electromagnetic field of strength \mathcal{E} that has typical frequency domain around the transition frequency ω of the two level system, with the interaction Hamiltonian

$$\hat{V} = \mathcal{E} d \sum_{n=1}^N \hat{\sigma}_{x,n}, \quad (2)$$

quantum transition among the states of the ensemble can occur. Here d denotes the transition dipole moment matrix element. Since the transition frequency ω belongs to the RF domain, with the typical wavelength exceeding the size of the atomic ensemble, all the atoms found themselves in the field of the same strength, which is therefore is placed in front of the summation.

The absorption spectrum of the ensemble with the energy spectrum of Fig.1 is depicted in Fig.2. On the

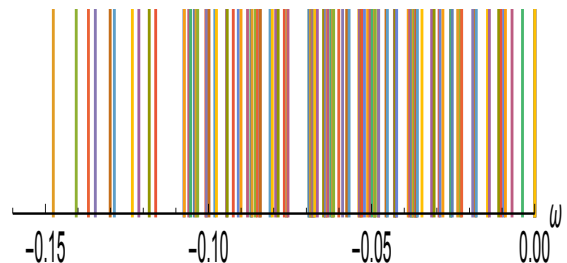


FIG. 2: Absorption spectrum of multiphoton transitions calculated for 7 atoms interacting via the second-order van der Waals coupling $1/R^6$ that are placed in a unit 3D box with periodic boundary conditions. The frequency axis (in arbitrary units) The multiphoton resonance corresponding to the minimal energy per atom is at the red side.

red side of the single-atom-single-photon transition frequency, one can find multiphoton resonances of different orders m , and among them one, located at the left edge of this multiphoton absorption spectrum. This very resonance corresponds to the transition to the state with the minimum energy per excited atom. Our aim to put our ensemble there.

However, the composite matrix element

$$V_m = \sum_{\text{all excitation channels}} \frac{(\mathcal{E}d)^m}{\prod_{\text{all intermediate detunings}} (k\hbar\omega - E_s)} \quad (3)$$

of the m -photon transition from the ground state to this multiply excited state of the ensemble should be very

small, such that the transition in question may require a very long time. For a classical-school multiphoton spectroscopist, the suggestion to carry out, say, a 100-photon transition in an ensemble of 200 atoms a might sound wild, – the Rabi frequency of such transition scales the intensity to the power of the half of the number of required excitations, and is an extremely small quantity. But in the Quantum Computation Science, the exponentially long lasting processes are rather usual things, the question is only in the minimization of the gross rate of the time required with the number of the two-level systems involved. If the energy position of the state to be populated is known, and there are no other state intervening the process, the situation can be considered as favorable, the Rabi transition period to the isolated target level scales as the square root of the total number of the states in the system, corresponding to the continuous analog of the Grover's search algorithm[12].

In a sense, performing a multiphoton transition of a very small amplitude, which does not require anything else but keeping coherence during a very long time, does not look as a process more difficult than keeping the coherence and performing in the same time a complicated control of a quantum computer required for realization of the Grover's computational algorithm. We therefore propose, if we may, to call "the Grover's time" the Rabi period of the transition to an isolated level of a complex spectrum of a quantum computer, while considering it as a process of multiphoton population of the eigenstates of time-independent Hamiltonian. The Grover's time is thus the parameter to be compared with another time parameter of a complex spectrum – the Heisenberg return time, given by the state density multiplied by the Planck constant, the time when one starts to distinguish discrete and continuous spectrum.

Generally speaking, the only condition which limits the selectivity of the transition to an isolated level is the time-energy uncertainty principle, – the transition time should not be shorter than the inverse size of the gap separating the target level from the other levels. Or in other words, the Grover's time has to be longer as compared to the Heisenberg time. Unfortunately, in the general case, one can hardly reach the such a regime where the excitation process conforms the model of multiphoton transitions between just two levels. There are at least two players that may intervene the process. First of all, there might be no sufficiently large energy gap separating the lowest in frequency resonance from the other levels. In this case, the population transfer may occur not to a single state, but to a large group of the states, each of which by itself is a rather good approximation to the required solution of the mathematical problem. However, dynamics of such a process is distinct from that of the two-level system and might result in broadening of the population distribution over the energy scale.

The second reason is coexistence of the weak highly multiphoton resonant transitions to the target levels at the absorption spectrum edge with strong but detuned

resonances corresponding to the states that are much more far from the edge but that are much stronger coupled to the ground state since they require less photons for the transitions. They also may spoil the width of the energy distribution making it much larger than this would be according to the energy-time uncertainty principle. To a certain extent, the role of such "spoiler" transitions can be reduced by employing Raman excitation scheme, as shown in Fig.3. By applying two exter-

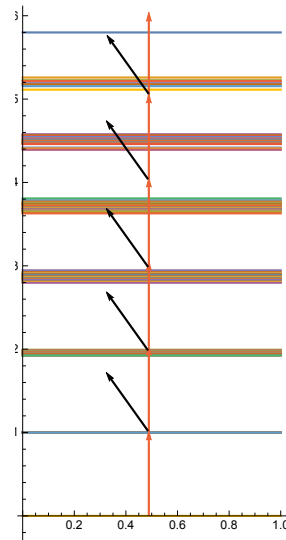


FIG. 3: Raman excitation of the band edges of the atomic ensemble permits to address the states with specified total number of the excited atoms. Virtual transitions induced by a strong blue-detuned field are shown by red arrows. Blue-detuned weak field induces transitions to a chosen edge of the spectrum (black arrows). In this figure, for the case of 7 atoms we show the regime where the number of excitations equals 3. For a larger atomic system, The edges of the states with the total number of excitations equal multiples of 3 will also be close to the Raman resonance.

nal fields, one detuned to the blue side, and the other detuned to the red side relative to the frequency of the single atom transition, one can specifically address the state of the ensemble with a chosen minimum number of the total excitations and the numbers of excitations given by multiples of this minimum number. In such a way, certain spoiler transitions can be moved far out from the resonance.

III. DYNAMICS OF A LEVEL-BAND SYSTEM.

We remind here the main features of the evolution of the level-band system and present some pictures helping to qualitatively understand meaning of the parameters responsible for different regimes. In the atomic units, the Schrödinger equation for a single level interacting with a

band of M levels reads

$$\begin{aligned} i\frac{\partial}{\partial t}\psi_0 &= E_0\psi_0 + \sum_{n=1}^M V_n\psi_n, \\ i\frac{\partial}{\partial t}\psi_n &= E_n\psi_n + V_n\psi_0, \end{aligned} \quad (4)$$

where the coupling matrix elements V_n are chosen real. For the initial condition $\psi_0(t=0) = 1$ imposed on the amplitude of the single level, and after taking direct and inverse Fourier transforms, Eq.(4) yields the exact solutions

$$\begin{aligned} \psi_0 &= \frac{1}{2\pi i} \int \frac{e^{-i\varepsilon t}}{\varepsilon - E_0 - \sum_{m=1}^M \frac{V_m^2}{\varepsilon - E_m}} d\varepsilon, \\ \psi_n &= \frac{1}{2\pi i} \int \frac{e^{-i\varepsilon t}}{\left(\varepsilon - E_0 - \sum_{m=1}^M \frac{V_m^2}{\varepsilon - E_m}\right)(\varepsilon - E_n)} d\varepsilon, \end{aligned} \quad (5)$$

with the integration contour going from $\varepsilon = -\infty + io$ to $\varepsilon = \infty + io$, where $o = +0$.

At times shorter than the Heisenberg return time given by the inverse of the mean band level spacing, according to the uncertainty principle, the summation can be replaced by integration. For a band infinitely broad in both positive and negative direction, assuming constant V_n one obtains

$$\begin{aligned} \sum_{m=1}^M \frac{V_m^2}{\varepsilon - E_m} &\rightarrow gV^2 \int \frac{dE_m}{\varepsilon - E_m} = -i\pi gV^2 \\ \psi_0 &= e^{-\pi gV^2 t} \\ \psi_n &= \frac{e^{-\pi gV^2 t} - e^{-iE_n t}}{E_0 - E_n - i\pi gV^2}, \end{aligned} \quad (6)$$

where g is the band state energy density. In other words, the level exponentially loses its population $\rho_0 = |\psi_0(t)|^2$ in accordance with the Fermi "golden rule" with rate $2\pi gV^2$. This population gets distributed among the resonant band levels following the Cauchy profile

$$\rho_n = \frac{1}{(E_0 - E_n)^2 + (\pi gV^2)^2}. \quad (7)$$

At the times shorter than the Heisenberg time, the discrete spectrum can be considered continuous. One can thus call it quasicontinuum. At the times longer than the Heisenberg times, replacement of the sum by the integral is not valid, and the exponential level decay no longer occurs. On the contrary, the population experiences recurrences – partially it returns back to the level and becoming of the order of the population of all other resonant levels it manifests fluctuations that depend on the specific positions of the band levels. The level even does not decay on average, when the Heisenberg return time is shorter than the Fermi golden rule decay time. This is the case of the couplings smaller than the average distance among the band energy levels.

Now the question arises – what happens to the essentially inhomogeneous band, when the couplings V can differ by orders of magnitudes for neighboring band levels? The average squared interaction and the average state density are no longer the parameters that govern the population dynamics. The reason for this is rather clear, – the main contribution to the mean square coupling may come from the rare strongly coupled band levels (the spoiler states) while the main contribution to the state density might come from the extremely weakly coupled states. In other words, the Fermi "golden rule" transition rates and the Heisenberg return times may differ drastically for the strongly and weakly coupled submanifolds of the band levels. This situation is illustrated in Fig.4 by an "eye-guiding" example of two potential pits with the spectra of the oscillatory motion, that can be accessed via tunneling from an excited state of a narrow potential pit.

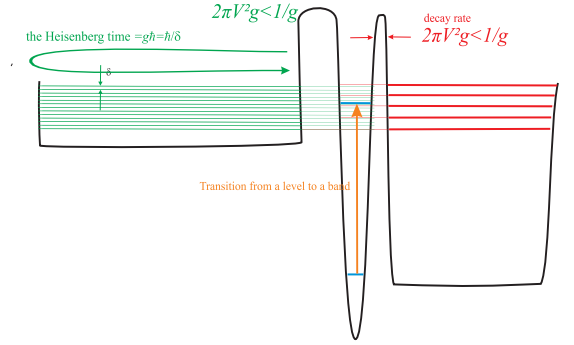


FIG. 4: Transition from a level to a band can be seen as the excitation of a quantum level in a narrow potential pit that can decay via tunneling to the domains of the periodic motions in other, broad, potential pits. Red levels in the narrower pit correspond to a shorter oscillation period, that is to a shorter Heisenberg return time, whereas the green levels correspond to a slower motion. Each pit represents the state with a given coupling size. The Fermi golden rule decay rate is proportional to the tunnel transparency of the barriers. If the periods of the motion in the broad pits corresponding to the Heisenberg return times are shorter than the decay rate, the decay does not occur. However, if there are many (not just two as in the picture) potential pits are available for the tunneling, the decay still may occur.

The situation may even turn out to be such, that non of many different submanifolds conforms the requirement of the "golden rule" applicability, and still all the submanifolds together will be able to accommodate all the level's population. One therefore needs to find suitable statistical characteristics of the band levels that govern the population dynamics and the energy distribution. One of the authors (V.A.) has considered such a problem in the context of multiphoton vibrational laser excitation of the polyatomic molecules[5], and (in collaboration) in the context of the excitation exchange in the ensemble of cold Rydberg atoms[11]. It seems expedient to briefly

remind the results, since a similar situation occurs at the quasicontinuum edge.

The band is considered as a manifold of levels randomly placed within a broad energy strip, with independent statistics of the level energy positions E_n and the sizes of the coupling matrix elements V_n . Moreover, position of each band level is assumed to be statistically independent from the positions of others. This assumption is very much different from the usual model of complex spectra, that conform models of Gaussian orthogonal, unitary or symplectic ensembles. However, for the situation of a complex system composed of the elements interacting via committing operators, which is the case of the Hamiltonian Eq.(1) with the interaction $F(\{\hat{\sigma}_{z,n}\})$, the model of the statistically independent level position uniformly distributed over an energy strip seems much more adequate, since the perturbation by commuting operators does not produce level "repulsion".

For the power-law statistics of the couplings $g(V) \sim V^{-\alpha}$, one can identify three different regimes of the level decay. For $\alpha < 2$ the expectation value of the number of resonances, the number of the band levels that satisfy the condition of the detuning smaller than the coupling is finite, $-\int V g(V) dV < \infty$. Therefore the number of band states accessible for the population transfer is finite, and the level does not decay completely. The transferred part of the level population is distributed among the levels with strong coupling. The main part of the dense but weakly coupled band levels remains unpopulated.

For $2 < \alpha < 3$ the level transfers its population completely, since the expectation number of resonances is infinite. The main contribution to this expectation value comes from the weakly bounded states, that at the end receive all the population of the level. However the process goes very slow, according not to the exponential, but to the power law $t^{-\beta(\alpha)}$. The population first goes to the strongly coupled levels, from where it is retrieved back to the isolated level after the corresponding Heisenberg time and is transferred further to a group of weaker coupled states. This population transfer continues toward yet weaker and weaker coupled band states with gradually decreasing velocity. For $\alpha > 3$ the process goes to the weakly coupled states, although the energy width of the population distribution is given by Eq.(7) in accordance with the Fermi "golden rule".

We now are going to consider similar processes at the quasicontinuum edge, paying attention to the energy distribution of the transferred population with the aim to make it located at the very edge of the spectrum and to be as narrow as it is suggested by the energy-time uncertainty principle.

IV. POPULATION DYNAMICS AT THE EDGE OF A UNIFORM QUASI-CONTINUUM SPECTRUM

Let us consider a Hamiltonian \hat{H}_0 with eigen states $|n\rangle$ that for $n > 0$ has homogeneous spectrum E_n of spectral density g located at the energy axis in the interval $[0, \Gamma]$ and an additional state $|0\rangle$ with the negative eigen energy E_0 . The state vector is given in terms of the state amplitudes as

$$|\psi(t)\rangle = \psi_0 |0\rangle + \sum_{n=1}^{n=N} \psi_n |n\rangle.$$

At times, shorter than the Heisenberg return time, we can consider the homogeneous spectrum as continuous, that is

$$\begin{aligned} \hat{H}_0 &= |0\rangle E_0 \langle 0| + \sum_{n=1}^{n=N} |n\rangle E_n \langle n| \\ &\simeq |0\rangle E_0 \langle 0| + \int_0^\Gamma |E\rangle E \langle E| g(E) dE. \end{aligned} \quad (8)$$

We assume that at time $t = 0$, the state $|0\rangle$ is fully populated, that is $\psi_0(t = 0) = 1$, and the interaction \hat{V} that couples the state $|0\rangle$ with the rest of the spectrum,

$$\hat{V} = \sum_{n=1}^{n=N} (|0\rangle V_{0n} \langle n| + |n\rangle V_{n0} \langle 0|) \quad (9)$$

$$\simeq \int_0^\Gamma (|0\rangle V_{0E} \langle E| + |E\rangle V_{E0} \langle 0|) dE. \quad (10)$$

with $V_{n0} = V_{0n}^*$, is switched on abruptly at this moment. For this case the state vector reads

$$|\psi(t)\rangle = \psi_0(t) |0\rangle + \int_0^\Gamma \psi_E(t) |E\rangle dE.$$

We first consider the transfer of population and its distribution $\rho_E(t) = |\psi_E(t)|^2$ at the red-edge of the uniform spectrum of the Hamiltonian H_0 after this switching, assuming also that the coupling elements are real and uniform, i.e., $V_{E0} = V$. Our aim is to understand how the presence of the edge modifies the population dynamics compared to the case of the infinite band. To this end we write the Schrödinger equation for the Fourier transforms $\psi_j(\varepsilon) = \int \psi_j(t) e^{i\varepsilon t} dt$ of the amplitudes $\psi_j(t)$ and arrive at the set of algebraic equations

$$\varepsilon \psi_0(\varepsilon) = E_0 \psi_0(\varepsilon) + \sum_{n=1}^N V \psi_n(\varepsilon) + 1 \quad (11)$$

$$\varepsilon \psi_n(\varepsilon) = E_n \psi_n(\varepsilon) + V \psi_0(\varepsilon). \quad (12)$$

One straightforwardly finds the solutions

$$\psi_0(\varepsilon) = \frac{1}{\varepsilon - E_0 + V^2 \sum_{m=1}^N \frac{1}{E_m - \varepsilon}} \quad (13)$$

$$\psi_n(\varepsilon) = \frac{V}{(\varepsilon - E_n) \left(\varepsilon - E_0 + V^2 \sum_{m=1}^N \frac{1}{E_m - \varepsilon} \right)} . \quad (14)$$

At this point, we make use of the fact that the time is short as compared to the Heisenberg return time and replace the sums by the integral

$$V^2 g \int_0^\Gamma \frac{1}{E - \varepsilon} dE = V^2 g (\log(\Gamma - \varepsilon) - \log(-\varepsilon)) \quad (15)$$

$$\simeq V^2 g (\log \Gamma - \log(-\varepsilon)) \quad (16)$$

where Γ has meaning of the cut-off energy limiting the size of the band affected by the interaction V . We also set $\log(\Gamma - \varepsilon) \approx \log(\Gamma)$. This assumption just results in a small deviation from precise results at short times (corresponding to large ε), but it considerably simplifies the calculations allowing one to ignore the contribution of the branching point at $\varepsilon = \Gamma$ when performing the inverse Fourier transformation. We denote $V^2 g = w$ and, define the positive quantity $\bar{E}_0 = -E_0 + w \log(\Gamma)$, thus arriving at

$$\psi_0(\varepsilon) = \frac{1}{\varepsilon - w \log(-\varepsilon) + \bar{E}_0} \quad (17)$$

$$\psi_E(\varepsilon) = \frac{V}{(\varepsilon - E) (\varepsilon - w \log(-\varepsilon) + \bar{E}_0)}, \quad (18)$$

which after the inverse Fourier transform yields the result

$$\psi_0(t) = \frac{1}{2\pi} \int_{-\infty+i0}^{\infty+i0} \frac{e^{-i\varepsilon t}}{\varepsilon - w \log(-\varepsilon) + \bar{E}_0} d\varepsilon \quad (19)$$

$$\psi_E(t) = \frac{1}{2\pi} \int_{-\infty+i0}^{\infty+i0} \frac{V e^{-i\varepsilon t}}{(\varepsilon - E) (\varepsilon - w \log(-\varepsilon) + \bar{E}_0)} d\varepsilon . \quad (20)$$

Now we turn to the calculation of the integrals of the inverse Fourier transformation. To assign the contour to the lower-half of the complex plane, we first set the branch-cut of the log function along the negative imaginary axis. The integration contour is shown in Fig.5. The pole for the integral in Eq.(19), is found to be the negative real number $\varepsilon_0 = -wW_0\left(\frac{e^{\bar{E}_0/w}}{w}\right)$ where $W_0(z)$ denotes the principal branch of the Lambert function, also known as product logarithmic function. The point ε_0 is the root of the integrand denominator. Residue calculus and the allowance for the contributions of the integrals along the branch cut result in

$$\psi_0(t) = -i \frac{e^{-i\varepsilon_0 t}}{1 - \frac{w}{\varepsilon_0}} - I , \quad (21)$$

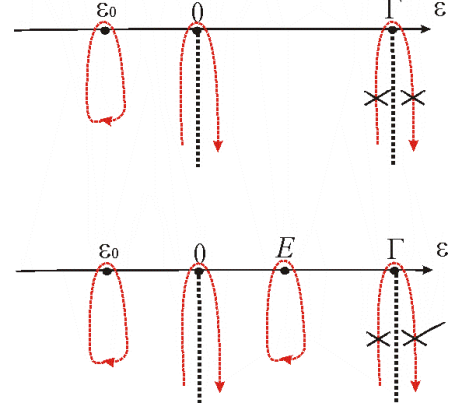


FIG. 5: Integration contours in the complex plane of ε (red curves) of the inverse Fourier transformation for ψ_0 (upper contour) and for ψ_E (lower contour). Dotted lines show cuts of the Riman surfaces starting at the logarithmic branching points; Contribution of the branching point at the upper edge of the band is ignored at times $t > 1/\Upsilon$.

where

$$I = \frac{i}{2\pi} \int_0^\infty \frac{e^{-yt}}{iy + w \log(y) + w \frac{i\pi}{2} - \bar{E}_0} dy - \frac{i}{2\pi} \int_0^\infty \frac{e^{-yt}}{iy + w \log(y) - w \frac{i3\pi}{2} - \bar{E}_0} dy . \quad (22)$$

By analogy, for the states in the quasi-continuum, Eq.(20), we obtain:

$$\psi_E(t) = -\frac{iV e^{-i\varepsilon_0 t}}{(\varepsilon_0 - E) \left(1 - \frac{w}{\varepsilon_0}\right)} - \frac{iV e^{-iEt}}{(E - w \log(-E) + \bar{E}_0)} - J, \quad (23)$$

where

$$J = \frac{iV}{2\pi} \left(\int_0^\infty \frac{e^{-yt}}{(iy + E) (iy + w \log y + w \frac{i\pi}{2} - \bar{E}_0)} dy - \int_0^\infty \frac{e^{-yt}}{(iy + E) (iy + w \log y - w \frac{i3\pi}{2} - \bar{E}_0)} dy \right) \quad (24)$$

Contribution of the poles give the asymptotic population for long times, while the contributions resulting from the integrals I and J along the cuts decrease with the time elapse. To overview the global time-dependence, in Fig. 6 (a) we present the time-evolution of isolated level population $|\psi_0(t)|^2$ for different parameters w and $|E_0|$, and where the integral I of Eq.(22) is performed numerically. The time dependence possess initially a fast stage with exponential decay (as for the case where the edges are absent) that is followed up by a regime of slower decay. To analytically identify the time dependence in the ‘slow’ regime we perform a change of variable, $u = yt$

in the integrals I and J in Eqs. (22) and (24) respectively. One then can see that the time dependence of the populations scales for long t as

$$|\psi_E(t)|^2 - |\psi_E(\infty)|^2 \sim (wt \log(wt))^{-1}. \quad (25)$$

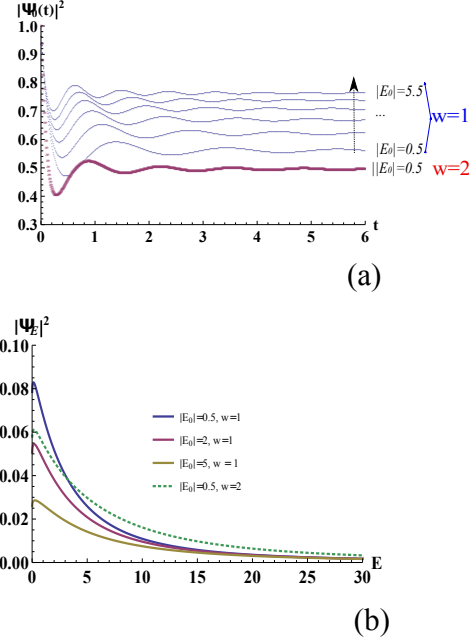


FIG. 6: (a) The decay of the population of the isolated level as a function of time. An exponentially fast decay rate is followed up by time domain of slower rate as described in Eq.(25). Asymptotically the population transferred to the continuum depends on the size of the gap $|E_0|$ and $w = gV^2$. (b) The distribution of the population over the energies of the continuum for sufficiently long times, $(wt \log wt)^2 \gg 1$. For the plot we have averaged out the fast oscillating interference/product term which results by taking the square magnitude of Eq.(23). We have employed the cut-off spectrum parameter $\Gamma = 40$.

Let us consider now the distribution of the transferred population in the regime of sufficiently long times, $(wt \log wt)^2 \gg 1$ where the contribution of the integrals I and J can be safely ignored. According to Eq.(23), the distribution of excited population over large energies E ,

$$\rho_n(t) = \frac{V^2}{(\varepsilon_0 - E_n)^2 (1 - \frac{w}{\varepsilon_0})^2} + \frac{V^2}{(E_n - w \log(-E_n) + \bar{E}_0)^2}, \quad (26)$$

scales as $1/E_n^2$ for large energies E_n . Note, that the population distribution profile is a superposition of two profiles with the inverse square dependence on the energy. Both of them correspond to the maxima at the negative energies, that is beyond the band, below the edge position. One of the profiles is centered at the position ε_0 , relatively close to the band edge, while the other is centered

close to the position of the isolated level energy \bar{E}_0 . The first profile, though it is scaled by the factor $(1 - \frac{w}{\varepsilon_0})^{-2}$, still may give a more significant contribution to the population at the quasicontinuum edge as compared to that of the second one. In Fig. 6 (b) distributions of population $|\psi_E|^2$ are plotted for different parameters and we observe that there is a clear maximum near the edge. According to numerical studies the width of the distribution follows an approximate dependence as $\sim w/|\bar{E}_0| = gV^2/|\bar{E}_0|$.

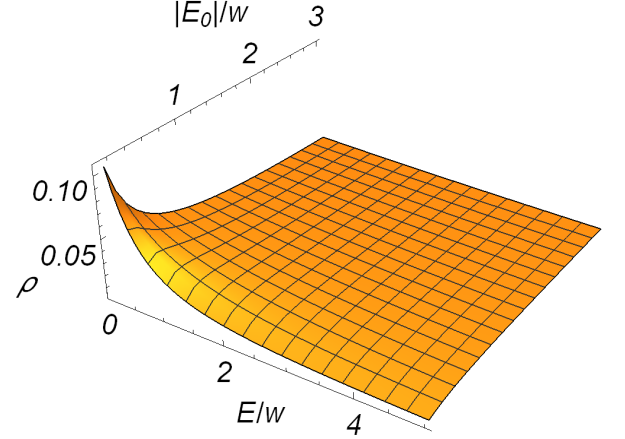


FIG. 7: The density of the transferred population part $\int_0^{\Gamma/100} |\psi_E|^2 dE$ as a function of the gap $|E_0|/w$ and the spectral position $|E|/w$ of the band levels next to the edge.

Let us summarize the results of the model of uniform quasicontinuum spectrum with edge and the abrupt switch-on of the interaction. After the switch-on, the population initially localized at the isolated level gets partially transferred to the quantum states at the continuum edge. Apart from the fast ($\sim e^{-wt}$) stage, the population transfer process has a slow and long lasting stage, where the time dependence of the population transfer turns out to be proportional to $(wt \log wt)^{-1}$. The total population transfer to the continuum is increased with increasing w and decreased with increasing gap $|E_0|$. The transferred population gets distributed over the states of the quasicontinuum according to the inverse square dependence with typical width $\sim w = gV^2$ corresponding to the time-energy uncertainty principle dictated by the fast stage. In Fig.7 one may overview the overall effect of w on the population transferred to the lowest part of the spectrum together with the effect of the gap. The uniform model in this simple setting, obviously does not provide much options for amplifying the population near the down edge. One should just bring the isolated level as near as possible to the edge ($|E_0| \ll 1$), choose weak couplings V , and wait for long enough time such as $(wt \log wt)^2 \gg 1$.

V. NON-ADIABATIC TRANSFER OF THE POPULATION.

The distribution width in the problem just considered is affected by the abrupt switch on of the interaction. The abrupt change of the interaction has the Fourier decomposition scaling as $1/\varepsilon$, and this is the very reason why the population distribution over energies behave as $1/E^2$. One therefore can address the question : "Is it possible to make this distribution narrower by avoiding abrupt switches?" At the first glance, one can think of the adiabatic increase of the interaction. However, in the regime of the highly multiphoton transitions, the adiabatic change is difficult to achieve, since any small and slow change of the electromagnetic field strength results in a much larger and faster change of the composite matrix element of the multiphoton transition Eq.(3). In contrast, by slow variation of the frequency of the electromagnetic field of a constant strength one may achieve a much more accurate control.

In order to understand the main features of the dynamics of the level-band system subject to the interaction with slowly changing frequency, we consider now the level-continuum edge problem in the rotating-wave approximation assuming the parabolic time-dependence of the level position. In other words $E_0(t) = E_o - \alpha t^2$, and whence the Schrödinger equation (4) for such a system takes the form

$$\begin{aligned} i\dot{\psi}_0 &= (E_o - \alpha t^2) \psi_0 + V \sum_{n=1}^{\infty} \psi_n, \\ i\dot{\psi}_n &= E_n \psi_n + V \psi_0. \end{aligned}$$

One can implement the Laplace contour integral method that suggest the time-frequency variable replacements

$$\begin{aligned} i\frac{\partial}{\partial t} &\rightarrow \varepsilon, \\ t &\rightarrow -i\frac{\partial}{\partial \varepsilon}, \end{aligned}$$

and obtain the Schrödinger equation of the form

$$\begin{aligned} \varepsilon \psi_0 &= E_o \psi_0 + \alpha \frac{\partial^2 \psi_0}{\partial \varepsilon^2} + V \sum_{n=1}^{\infty} \psi_n \\ \varepsilon \psi_n &= E_n \psi_n + V \psi_0, \end{aligned}$$

which yields the equation

$$\alpha \frac{\partial^2 \psi_0}{\partial \varepsilon^2} = \left(\varepsilon - \sum_{n=1}^{\infty} \frac{V^2}{\varepsilon - E_n} - E_o \right) \psi_0 \quad (27)$$

for the isolated level.

In Eq.(27) one recognizes the Schrödinger equation of a one-dimensional quantum particle moving along the "coordinate" ε in the "external potential" $\varepsilon - \sum_{n=1}^{\infty} \frac{V^2}{\varepsilon - E_n}$

with the total "energy" E_o , and therefore at times shorter then the Heisenberg time, the problem of the quasi-continuum edge excitation in the conditions of a parabolic time dependence of the detuning can be mapped to the problem of the scattering by the potential

$$\begin{aligned} \varepsilon - \sum_{n=1}^{\infty} \frac{V^2}{\varepsilon - E_n} &\rightarrow \varepsilon + w \int_0^{\Gamma} \frac{1}{E - \varepsilon} dE \\ &\rightarrow \varepsilon + w \log(-\varepsilon) \end{aligned}$$

where the last replacement also imply the energy scale shift $E_o \rightarrow E_o + w \log(\Gamma)$, same as earlier.

The Schrödinger equation also contains a contribution resulting from the level motion, – it has the form of "kinetic energy" with the parameter α characterizing the rate of the parabolic approach to the minimum detuning E_o playing role of the inverse mass of the scattered particle. Still, there is one important difference between such a "scattering" problem and the regular scattering process – the potential has an imaginary part, which allows for the possibility of absorption of the scattering particle for the positive coordinates.

We solve Eq.(27) numerically and calculate the probability profile $|\psi_0(\varepsilon)|^2$ for specific values of the parameters E_o/w and α/w^2 . In Fig.8 we present the results of the calculation. As one can see, that the oscillations observed for negative values of the "coordinate" ε , fade away for the positive coordinates. The profile resembles Airy function, and indeed, for large detunings, that is large negative parameters E_o/w , the profile is given by the absolute value of the square of the Airy function, which is simply the Fourier decomposition of a signal of constant amplitude with the parabolic frequency modulation. No absorption occur in this limit.

For decreasing minimum detuning, the exponential "tail" of the population profile corresponding to the classically forbidden domains, starts to reach the positive values of the coordinate, where the population can be "absorbed", that is transferred to the edge states of the continuum. The "incident" and the "reflected" waves no longer have equal amplitudes, and the profile $|\psi_0(\varepsilon)|^2$ no longer reaches zero values for the negative coordinate, as it is shown in Fig. 9. Some part A of the "incident amplitude" is absorbed. The total fraction of the population transferred to the band amounts to this very value. In Fig.10 we show the nonadiabatic transition probability found with the help of the WKB method and numerically, respectively, as a function of the parameters E_o/w and α/w^2 by solving the Schrödinger equation (27) for scattering. For comparison we also show the same quantity found with the help of the semiclassical formula

$$\exp \left\{ - \int_{W_0(e^{-E_o/w})}^0 \sqrt{\frac{\varepsilon + V^2 g \log(-\varepsilon) - E_o}{\alpha}} d\varepsilon \right\}, \quad (28)$$

with the lower integration limit given by the Lambert

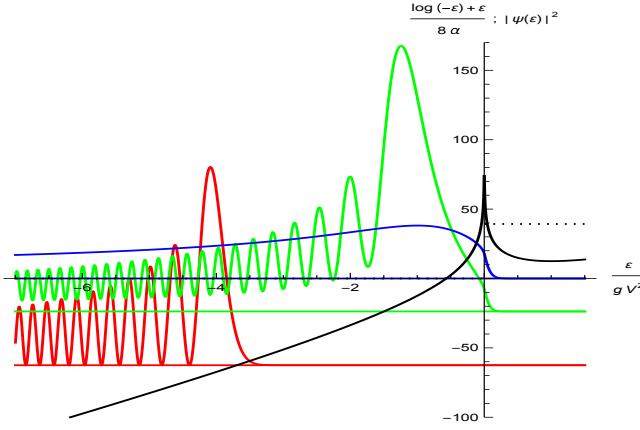


FIG. 8: Non-adiabatic transition to the continuum edge as a scattering problem in the presence of absorption. The scattering potential (solid black curve) and the absorption profile (dotted line) result in the probability profile depending on the "energy" of the scattered particle, which corresponds to the minimum size E_o of the gap between the level and the continuum edge. For big gaps, (negative "energies") the "absorption", that the probability transition to the continuum edge is negligible, and the distribution is given by the Airy function (red curve). For small gaps the absorption is important and the incident and back-scattered waves have different amplitudes (green curve). For close approach, the nonadiabatic transfer is complete (blue curve) and no "back scattered" amplitude is longer seen. The closer sets one the "classical turning point" to the continuum edge, the broader is the energy distribution of the absorbed population. By an optimum choice of the "mass" α^{-1} , the distribution can be minimized to the limit suggested by the uncertainty principle.

function. One sees, that in the case the level slowly approaches the continuum edge, the nonadiabatic transition probability can be rather high if $W_0 (e^{-E/w})$ is close enough to zero.

At the same time, the width of the population distribution may remain narrow, since the integrand in Eq.(28) remains large for positive ε . In Fig.11 we show the inverse width of the transferred probability distribution found numerically as a function of the same parameters E_o/w and α/w^2 .

One sees, that by a proper choice of the size of these parameters it is possible to obtain a narrow energy distribution of the continuum edge, while the probability of the non-adiabatic transition remains of the order of unit. The distribution width, and the typical time $\sim 1/\sqrt{\hbar\alpha}$ required for such a process are related by the saturation limit of the time-energy uncertainty principle. Actually, the optimum regime corresponds to a very slow (small α) approach to the maximum energy E_o , which takes a positive value. Specific values of E_o and α can be numerically found for each predetermined probability of transition and each given size of the required width.

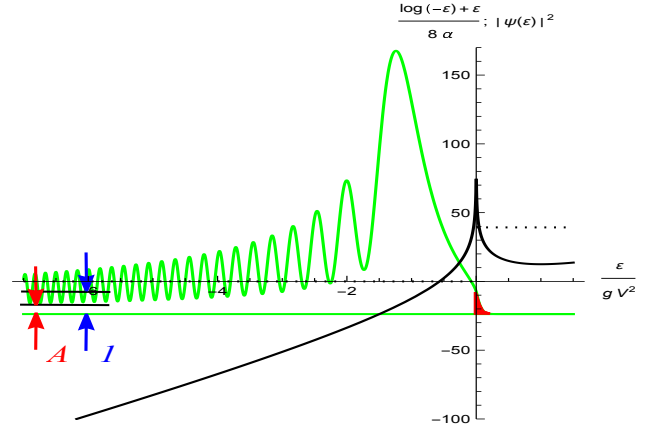


FIG. 9: "Back scattered amplitude" differs from the incident amplitude due to the absorption. The difference A allows one to find numerically the amount of the population, which has been transferred non-adiabatically from the moving isolated level to the band. This part corresponds to the red filled profile.

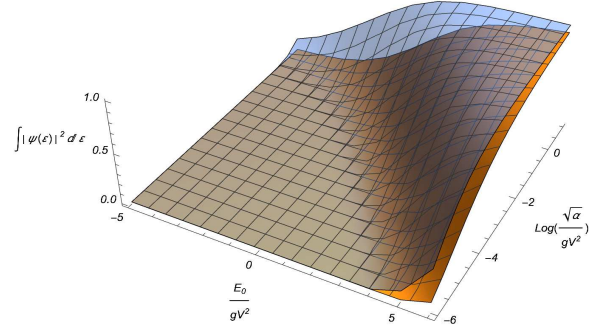


FIG. 10: Probability of the nonadiabatic transition to the states at the continuum edge calculated with WKB method (blue surface) and calculated numerically (yellow surface) as functions of the minimum energy gap parameter E_o/gV^2 and the approach rate parameter $\alpha/(gV^2)^2$.

VI. POPULATION OF THE QUASICONTINUUM EDGE IN THE PRESENCE OF A SINGLE SPOILER STATE

The assumption of homogeneously distributed couplings over the quasicontinuum does not look as a satisfactory model of the real spectra of multiphoton transitions in ensembles of interacting atoms, – neighboring states may correspond to different orders of the multiphoton resonances and their composite matrix elements may be drastically different. In fact, the spectral density of the low-order resonances with high couplings has to be much smaller as compared to the that for the much more abandoned and weakly coupled high-order resonances.

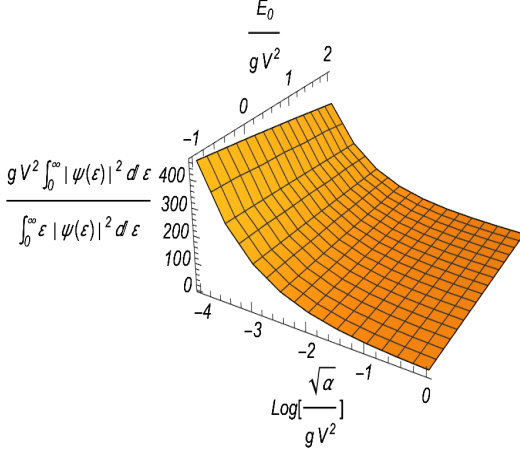


FIG. 11: The inverse width of the probability energy distribution near the continuum edge as function of the minimum energy gap parameter E_0/gV^2 and the approach rate parameter $\alpha/(gV^2)^2$.

In this Section, we make a first simple modification of the homogeneous spectrum model. We assume the existence of a ‘spoiler’ state $|S\rangle$ of energy E_s , with $0 < E_s < \Gamma$, whose coupling to the ground state is much stronger than the average coupling, i.e., $|V_{s0}| = |V_s| \gg |V|$. We separately study the amplitude of the spoiler state $\psi_S(t)$ and modify Eqs.(19)-(20) as:

$$\psi_0(t) = \int_{-\infty+i0}^{\infty+i0} \frac{d\varepsilon}{2\pi} \frac{e^{-i\varepsilon t}}{\varepsilon - w \log(-\varepsilon) + \bar{E}_0 + \frac{|V_s|^2}{E_s - \varepsilon}} \quad (29)$$

$$\psi_E(t) = \int_{-\infty+i0}^{\infty+i0} \frac{d\varepsilon}{2\pi} \frac{V e^{-i\varepsilon t}}{(\varepsilon - E) \left(\varepsilon - w \log(-\varepsilon) + \bar{E}_0 + \frac{|V_s|^2}{E_s - \varepsilon} \right)} \quad (30)$$

$$\psi_{E_s}(t) = \int_{-\infty+i0}^{\infty+i0} \frac{d\varepsilon}{2\pi} \frac{V_s e^{-i\varepsilon t}}{(\varepsilon - E_s) \left(\varepsilon - w \log(-\varepsilon) + \bar{E}_0 - |V_s|^2 \right)} \quad (31)$$

where it is implicit that $\psi_E = \psi_{E \neq E_s}$.

As earlier, in order to calculate the integrals, we perform contour integration at the complex plane. We start with the ground state amplitude $\psi_0(t)$, for which the integrand denominator has two roots to be found numerically: a real root $\varepsilon_1 < 0$ and a complex root ε_2 which has positive real part and (small) negative imaginary part. The integration contour as shown in Fig.12 We integrate on the complex plane along a path that is slightly upper than the real axis and that goes around the branch cut of the log-function – which is placed as before along the negative imaginary axis. Thus both residues, corresponding to the roots $\varepsilon_{1,2}$ need to be taken into account,

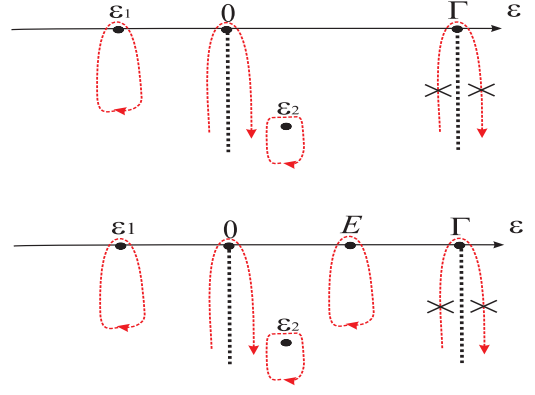


FIG. 12: Integration contours for the level (upper) and the band state (lower) amplitudes in the presence of a spoiler state with the energy E_s .

arriving at:

$$\psi_0(t) = -i \sum_{k=1}^2 \frac{e^{-i\varepsilon_k t}}{1 - \frac{w}{\varepsilon_k} + \frac{|V_s|^2}{(E_s - \varepsilon_k)^2}} - L, \quad (32)$$

where

$$L = \int_0^\infty \left(\frac{ie^{-yt}}{iy + w \log(y) + \frac{i\pi w}{2} - \bar{E}_0 - \frac{|V_s|^2}{E_s + iy}} \right) dy \quad (33)$$

$$- \frac{ie^{-yt}}{iy + w \log(y) - \frac{i3\pi w}{2} - \bar{E}_0 - \frac{|V_s|^2}{E_s + iy}} \frac{dy}{2\pi}. \quad (34)$$

The two regimes of the time-evolution of the population of the ground state persist in the presence of the spoiler state, see Fig 13 (a), while there is an additional weak exponential decay due to ε_2 that is not evident in this figure. We proceed with deriving the population transferred to the continuum, excluding the part ‘absorbed’ by the spoiler state. Here, we include the additional to $\varepsilon_{1,2}$, positive pole E and arrive at:

$$\psi_E(t) = \frac{-iV^* e^{-iEt}}{\left(E - w \log(-E) + \bar{E}_0 + \frac{|V_s|^2}{E_s - E} \right)} \quad (35)$$

$$- \sum_{k=1}^2 \frac{iV^* e^{-i\varepsilon_k t}}{(\varepsilon_k - E) \left(1 - \frac{w}{\varepsilon_k} + \frac{|V_s|^2}{(E_s - \varepsilon_k)^2} \right)} - M, \quad (36)$$

where

$$M = \int_0^\infty \frac{e^{-yt}}{iy + E} \left(\frac{iV^*}{iy + w \log y - \frac{i3\pi w}{2} - \bar{E}_0 - \frac{|V_s|^2}{E_s + iy}} - \frac{iV^*}{iy + w \log y + \frac{i\pi w}{2} - \bar{E}_0 - \frac{|V_s|^2}{E_s + iy}} \right) \frac{dy}{2\pi}.$$

Finally we provide the population of the spoiler state

where we have only the contribution of the two poles $\varepsilon_{1,2}$,

$$\psi_{E_s}(t) = \sum_{k=1}^2 \frac{-iV_s^* e^{-i\varepsilon_k t}}{(\varepsilon_k - E) \left(1 - \frac{w}{\varepsilon_k}\right) + \varepsilon_k - \log(-\varepsilon_k) + \bar{E}_0} - P, \quad (37)$$

where

$$P = \int_0^\infty \left(\frac{iV_s^* e^{-yt}}{(iy + E_s)(iy + w \log y - \frac{i3\pi w}{2} - \bar{E}_0) - |V_s|^2} - \frac{iV_s^* e^{-yt}}{(iy + E_s)(iy + w \log y + \frac{i\pi w}{2} - \bar{E}_0) - |V_s|^2} \right) \frac{dy}{2\pi}. \quad (38)$$

$$(39)$$

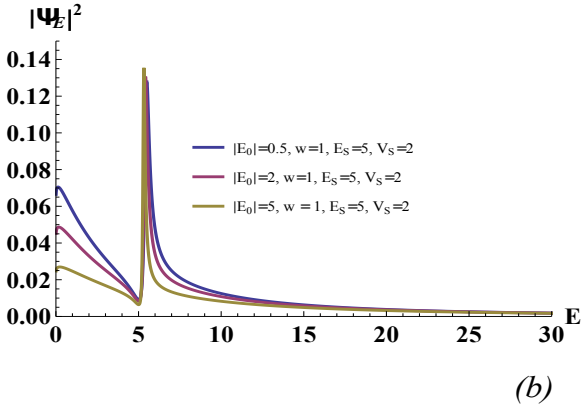
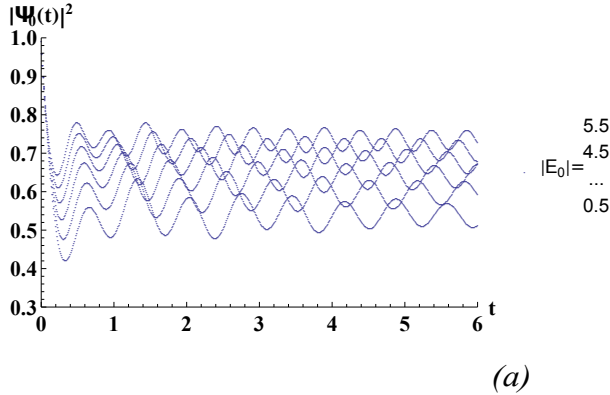


FIG. 13: hh

From the plots in Fig. 13 (b) (and by comparison to those of Fig. 6) we may observe that the presence of the spoiler state does not have a considerable impact on the shape of the distribution at the “bottom” of the continuum where we are interested in. Still a more detailed numerical study shows that there is an increase of the population at the bottom-edge as the energy E_s spoiler state is approaching the down edge. This is explained by the Fano-type profile in the distribution, see Fig. 13 (b), where the band states near the spoiler state get populated and the population has a “tail” directed to the side

of higher energies. We note here that the ‘Fano’ profile appearing in our case study is due to the *indirect* interaction of the spoiler state with the band levels via the isolated level, and not due to the direct interaction as in the original problem investigated by Fano.

VII. SPOILER STATE IN THE CASE OF THE NONADIABATIC POPULATION TRANSFER.

Now the effect of the spoiler state for the case of slowly moving level. The Schrödinger equation takes the form:

$$\alpha \frac{\partial^2 \psi_0(\varepsilon)}{\partial \varepsilon^2} = \left(\varepsilon - E_o - \int \frac{1}{\varepsilon - E_n} dE_n - \frac{|v_s|^2}{\varepsilon - E_s} \right) \psi_0(\varepsilon),$$

and the new scattering potential now includes two more parameters – the energy position E_s of the spoiler state, and its “force” $|v_s|^2$. The typical shape of the population distribution $|\psi_0(\varepsilon)|^2$ following from the numerical solution of this equation has the form depicted in Fig.14. As

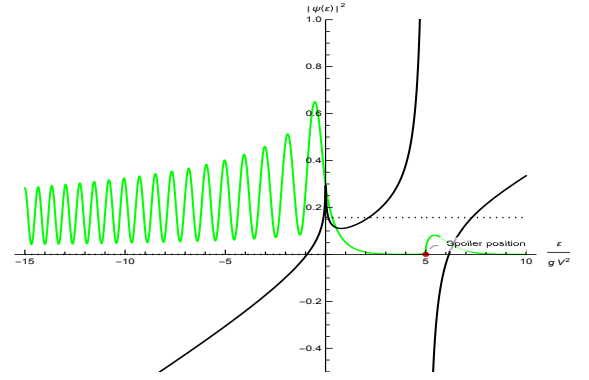


FIG. 14: Numerical solution of the Schrödinger equation (green curve) yields the population distribution, that apart of the populated domain near the quasicontinuum edge, contains the part located in the vicinity of the spoiler state $E_s = 5w$, $V_s = w\sqrt{5}$. The spoiler modifies the “scattering potential” (solid black curve for the real part and dotted black line for the imaginary part) and creates a “classically allowed” domain at the blue side of it’s energy position.

one sees, a fairly strong spoiler significantly changes the population distribution profile. The main effect is due to the change of the “scattering potential”, – next to the spoiler, it may result in a “classically allowed” domain, which takes an appreciable fraction of the population.

Two questions should be answered now: (i) How does the spoiler presence affect the width of the distribution near the continuum edge? and (ii) How large is the fraction of the population that has been moved in the vicinity of the spoiler state? We start with the first question and find numerically the dependence of the inverse of the edge population width as a function of the parameters E_s and

$|v_s|^2$. In Fig.15 we depict the results found for the spoiler parameters $|E_0| = 9gV^2$ and $\alpha = 10^{-2} (gV^2)^2$.

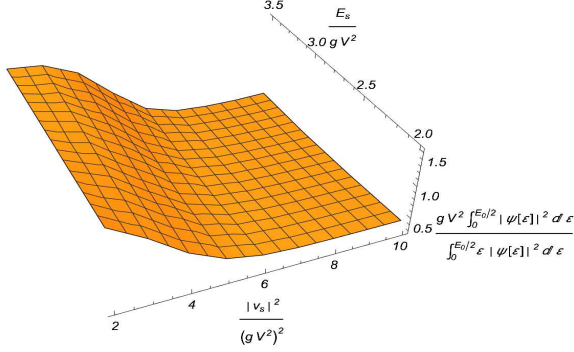


FIG. 15: Dependence of the population distribution inverse width at the the edge as function of the parameters E_s and $|v_s|^2$ for $|E_0| = 5gV^2$ and $\alpha = (gV^2)^2$.

In Fig.16 we depict the inverse of the population distribution width as function of the parameters α and $|v_s|^2$ for $|E_0| = 9gV^2$ and $E_s = 8.7gV^2$. One can see that even in the presence of a spoiler, the slower the approach rate α to the continuum is, the narrower the distribution. As compared to the case of the abrupt "switch on", one can gain narrowing by orders of magnitude.

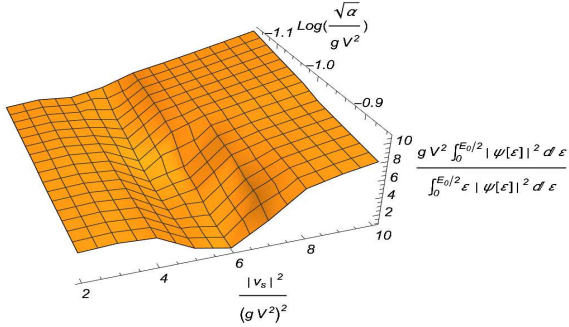


FIG. 16: Dependence of the population distribution inverse width at the the edge as function of the parameters α and $|v_s|^2$ for $|E_0| = 5gV^2$ and $E_s = 2gV^2$.

Answering the second question, we numerically consider the ratio of the total population of the continuum edge and the total population in the vicinity of the spoiler. In Fig.17 we present the result of the calculation in function of the spoiler strength $|v_s|^2 / (gV^2)^2$ and the adiabaticity parameter $\sqrt{\alpha}/gV^2$. In Fig.18 we present the dependence of the ratio between these populations as a function of the position of the spoiler state in energy and the spoiler strength. One sees, that the overall population near the spoiler state gets smaller then the

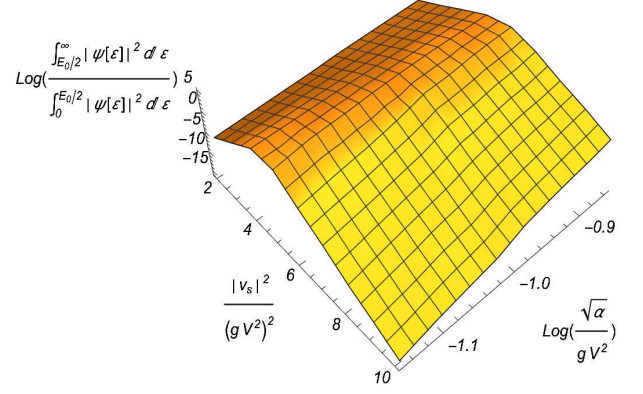


FIG. 17: Ratio of the total population of the continuum edge and the total population in the vicinity of the spoiler as a function of the spoiler strength $|v_s|^2 / (gV^2)^2$ and the adiabaticity parameter $\sqrt{\alpha}/gV^2$, for $|E_0| = 5gV^2$ and $E_s = 2gV^2$. The plane corresponds to equal populations at the edge and around the spoiler.

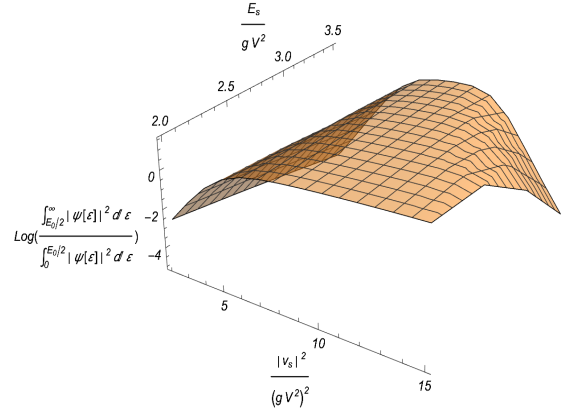


FIG. 18: Ratio of the total population of the continuum edge and the total population in the vicinity of the spoiler as a function of the spoiler strength $|v_s|^2 / (gV^2)^2$ and the spoiler position E_s/gV^2 for the adiabaticity parameter $\sqrt{\alpha}/gV^2 = 1$ and for $|E_0| = 5gV^2$. The plane corresponds to equal populations at the edge and around the spoiler.

approach rate α decreases, in complete agreement with the Landau-Zener result for the nonadiabatic transition in a two-level system, with the only difference, that the population does not stay in the spoiler state itself, but gets redistributed among the band levels in its vicinity following the profile of Fig.14.

VIII. NUMEROUS SPOILER STATES, STATISTICAL DESCRIPTION.

Presence of a single spoiler state changes the energy distribution of the population. In spite of the fact that the spoiler state by itself does not have significant population in the long time limit, it leads to appreciable population of the neighboring weakly coupled states of the quasicontinuum. For the abrupt switch-on of the interaction, the populated states mainly locate on the "blue" side, that is at the energies larger relative to the spoiler state energy, while for the adiabatic case, the situation is opposite – the populated states are on the red side, as one can see in the figures above. The natural question arises: what kind of the population distribution attains when there are many spoiler states?

Expression (5) for the Fourier transform of the amplitude (14) of the quasicontinuum state n

$$\psi_n(\varepsilon) = \frac{1}{\left(\varepsilon - E_0 - \sum_{m=1}^M \frac{V_m^2}{\varepsilon - E_m}\right) (\varepsilon - E_n)},$$

remains valid in this case, but the replacement of the sum by the integral no longer can be performed. In order to understand the reason for this, let us assume that there are many spoiler states with different sizes of couplings V_k , that are irregularly distributed over the band with energies E_{m_k} . The total number of the spoilers with a given V_k is M_k . We therefore rewrite the sum in the denominator regrouping the spoiler states of the same size of interaction

$$\sum_{n=1}^M \frac{V_m^2}{\varepsilon - E_m} \rightarrow \sum_k V_k^2 \sum_{m_k=1}^{M_k} \frac{1}{\varepsilon - E_{m_k}}.$$

The Heisenberg return time for each of the sums $\sum_{m_k=1}^{M_k} \frac{1}{\varepsilon - E_{m_k}}$ is given by the spectral density of the spoilers of this type, and is much shorter than the Heisenberg return time of the entire spectrum. This implies, that each group of M_k spoiler states, after having initially absorbed a certain amount of the population of the ground state 0, returns it back, and this returned population is further redistributed over the other states of the band. This process is neither adiabatic nor abrupt, but occurs with a certain (rather complicated) time dependence characterized by a typical time scale specific for the energy spectrum E_{m_k} of the group under consideration.

No consistent statements can be done in the general case of a complex specific distribution of the spoiler states. Still, one can consider an average behavior of such systems by making an assumption about statistical distribution of the spoilers, that is tackling the problem following the Wigner's idea of ensemble average. However, the Gaussian statistical ensembles, traditionally employed as models of complex spectra, imply chaotic quantum dynamics of the system with completely destroyed quantum numbers of the parts comprising the system, which is not the case for the problem under consideration. In fact,

in the situation under consideration, each eigen state of the quasicontinuum corresponds to the tensor product of the individual states of two-level atoms. Therefore, we choose as model the opposite extreme and assume, that the energy position of each spoiler state is statistically independent of the positions of other spoilers.

Performing the statistical description, one can no longer consider the state amplitudes, since the ensemble average results in the average of their phases and thus completely destroys all the information about state populations. The ensemble average has to be done for the populations, which we write in the form

$$\langle \rho_n(\varepsilon, \xi) \rangle = \left\langle \frac{1}{\left(\varepsilon - E_0 - \sum_{m=1}^M \frac{V_m^2}{\varepsilon - E_m}\right) (\varepsilon - E_n)} \frac{1}{\left(\xi - E_0 - \sum_{m=1}^M \frac{V_m^2}{\xi - E_m}\right) (\xi - E_n)} \right\rangle, \quad (40)$$

where the angular brackets denote the averaging. After the Fourier transformation, multiplication by the factor $e^{-i(\varepsilon - \xi)t}$ and integration over ε and ξ from $-\infty \pm 0i$ to $\infty \pm 0i$ with the upper sign corresponding to ε and the lower to ξ , this expression will give the time dependent ensemble average population of the state n .

In order to perform the ensemble average for the semi-infinite inhomogeneous band, we employ the same procedure as has been earlier done [5] for the infinite band, by rewriting the fractions in Eq.(40) with the help of two auxiliary variables τ and θ as the Laplace images of the exponents

$$\langle \rho_n(\varepsilon, \xi) \rangle = \int_0^\infty \left\langle \frac{e^{i\tau(\varepsilon - E_0 - \sum_{m=1}^M \frac{V_m^2}{\varepsilon - E_m})}}{\varepsilon - E_n} \frac{e^{-i\theta(\xi - E_0 - \sum_{m=1}^M \frac{V_m^2}{\xi - E_m})}}{\xi - E_n} \right\rangle d\tau d\theta, \quad (41)$$

allowing the factorization

$$\langle \rho_n(\varepsilon, \xi) \rangle = \int_0^\infty \frac{e^{i\tau(\varepsilon - E_0) - i\theta(\xi - E_0)}}{(\varepsilon - E_n)(\xi - E_n)} \prod_{m=1}^M \left\langle e^{\frac{i\theta V_m^2}{\xi - E_m} - \frac{i\tau V_m^2}{\varepsilon - E_m}} \right\rangle d\tau d\theta. \quad (42)$$

Let us concentrate now at the energy average for each individual level

$$\left\langle e^{i\left(\frac{\theta V_m^2}{\xi - E_m} - \frac{\tau V_m^2}{\varepsilon - E_m}\right)} \right\rangle = \frac{1}{\Gamma} \int_0^\Gamma e^{i\left(\frac{\theta V_m^2}{\xi - E_m} - \frac{\tau V_m^2}{\varepsilon - E_m}\right)} dE_m$$

randomly distributed within a broad energy band $(0, \Gamma)$, with $\Gamma \rightarrow \infty$. Note, that actually, the width can be set to infinity, it just requires to take into account some

logarithmic change of the level energy $E_0 \rightarrow \bar{E}_0$, similar to the case of the homogeneous band. The argument of the exponent tends to zero with increasing energy, and hence the integrand is close to unity in the most part of the integration interval. Therefore the average is very close to unity and one can write

$$\left\langle e^{\frac{i\theta V_m^2}{\xi - E_m} - \frac{i\tau V_m^2}{\varepsilon - E_m}} \right\rangle \simeq e^{\frac{1}{\Gamma} \int_0^\Gamma \left(e^{\frac{i\theta V_m^2}{\xi - E} - \frac{i\tau V_m^2}{\varepsilon - E}} - 1 \right) dE}.$$

The expression obtained allows one to explicitly write the product of the contribution of the individual levels Eq.(42) in the form of the sum in the exponent replaced by the integral

$$\prod_{m=1}^M \left\langle e^{i \left(\frac{\theta V_m^2}{\xi - E_m} - \frac{\tau V_m^2}{\varepsilon - E_m} \right)} \right\rangle \rightarrow e^{\int_0^\Gamma dE \int dV g(V) \left(e^{\frac{i\theta V^2}{\xi - E} - \frac{i\tau V^2}{\varepsilon - E}} - 1 \right)},$$

where $g(V)$ stands for the spectral density of the states of the band levels with the coupling V . We finally obtain the equation

$$\begin{aligned} \langle \rho_n(t) \rangle &= V_n^2 \int_{-\infty+i0}^{\infty+i0} d\varepsilon \int_{-\infty-i0}^{\infty-i0} d\xi e^{-i(\varepsilon-\xi)t} \\ &\int_0^\infty d\tau d\theta \frac{e^{i\tau(\varepsilon-E_0) - i\theta(\xi-E_0) + F}}{(\varepsilon - E_n)(\xi - E_n)} \end{aligned} \quad (43)$$

which represents the population distribution over the band in the form of the four-fold integral, while all the information about the behavior of the system is contained in the function

$$F(\varepsilon, \xi, \theta, \tau) = \int_0^\Gamma dE \int dV g(V) \left(e^{\frac{i\theta V^2}{\xi - E} - \frac{i\tau V^2}{\varepsilon - E}} - 1 \right). \quad (44)$$

We just note that for the first, linear, term of the Taylor expansion of the exponent over V^2 , the contribution of the upper limit Γ can be included, as earlier, to the energy \bar{E}_0 of the isolated level, while for all higher terms the upper integration limit can be directly set to infinity. With this remark, we consider Γ to be infinite hereafter, unless the allowance of the finite size of this quantity is essential indeed.

IX. INTERMEDIATE TIME ASYMPTOTIC FOR THE POPULATION DISTRIBUTION.

Analytic calculation of a four-fold integral Eq.(43) of the general type of F given by Eq.(44) is not something one can easily do. Even performing an approximate calculation with the stationary point method, one may encounter difficulties in the case where the stationary points are not parabolic. Therefore, our aim now is to find

a regime where some consistent statements still can be done.

We first note, that in contrast to the regime, where the couplings V can be considered as small, such that the Taylor expansion of the Eq.(44) in V^2 returns us back to the model of the uniform band considered in Sec.IV, for the case of strongly coupled spoiler states, we have to identify another regime, where V^2 are considered not perturbatively. For this case, one can employ the Taylor expansion in the population frequency instead of the couplings.

This regime turns out to be an intermediate time asymptotic, where the time is much longer than the Grover's time, but still very short as compared to the Heisenberg return time of the entire system. This implies that the time is sufficiently long to ensure transition to any isolated level of the band, but still does not allow yet to see the levels as individual and isolated. In other words, for the regime where $Vg \gg 1$, we consider the time $\hbar/V \ll t \ll \hbar g$. Note that the parameter Vg is encountered in many fields of the quantum physics, it's square is known as the "conductance" in the superconductivity theory, and the requirement $Vg \gg 1$ is known as the quasicontinuum existence condition in the field of laser-matter interaction.

The main idea of the calculation is as follows. Since we consider the asymptotic of times long compared to the Heisenberg time, where the population changes slowly, we assume that the difference ζ between variables ε and ξ in Eq.(43), corresponding to the typical frequencies of the population distribution time variation, to be small, and therefore we cast the average Eq.(44) in the first order Taylor series over ζ and write

$$F(\varepsilon, \xi, \theta, \tau) = G\left(i\frac{\theta - \tau}{\eta}\right) + i\zeta \frac{\theta + \tau}{2} J\left(i\frac{\theta - \tau}{\eta}\right). \quad (45)$$

Here $\eta = \frac{\varepsilon + \xi}{2}$, while the Taylor coefficients are the functions

$$\begin{aligned} G\left(i\frac{\theta - \tau}{\eta}\right) &= \int_0^\Gamma dE \int dV g(V) \left(e^{\frac{i(\theta - \tau)V^2}{\eta - E}} - 1 \right) \\ J\left(i\frac{\theta - \tau}{\eta}\right) &= \int_0^\infty dE \int dV \frac{g(V) V^2 e^{\frac{i(\theta - \tau)V^2}{\eta - E}}}{(\eta - E)^2}, \end{aligned}$$

that have to be found for a specific choice of the coupling matrix elements statistics model. Now ζ and η are our new integration variables replacing ε and ξ .

Note, that the expansion Eq.(45) is legitimate only for the negative values of η that does not lead to singularities in the exponent in Eq.(44) on the integration interval, while the positive part of η axis yields a contribution decaying with time, similar to that of the quasicontinuum infinite in both sides. In other words, in Eq.(26), the inhomogeneity of the band affects the first and the second contributions in a different way, – the first one gets shifted along the real direction of the energy axis,

while the second acquires a decreasing time dependence. We will not consider the role of the latter here in detail, but just illustrate this general feature in a tractable toy example presented in the next Section.

In this regime of small ζ we also note, that smallness of ζ implied by the long time asymptotic also implies a large typical size of the sum $y = \theta + \tau$, which therefore scales as time t , in contrast to a typical size of the variable difference $x = \theta - \tau$, remaining of the order of $1/gV^2$. This allows one to lift up the constrain $|\theta - \tau| < |\theta + \tau|$ dictated by the requirement $\theta, \tau > 0$ and perform integration over y and x independently. The integration over dy yields a pole at $\zeta = 0$, and the contribution of this pole to the integral over $d\zeta$ yields the time independent density distribution in the form of a two-fold integral

$$\langle \rho_n \rangle = \int_{-\infty}^0 d\eta \int_{-\infty}^{\infty} dx \frac{V_n^2 e^{-ix(E_o - \eta) + G(x/\eta)}}{(\eta - E_n)^2 (1 - J(x/\eta))}. \quad (46)$$

In a cases of large $G(x/\eta)$ where the integral Eq.(46) can be evaluated with the saddle point method, the saddle point for η gives the position of a "factive" level which replaces the displaced position ε_0 of the isolated level entering the expression Eq.(26) for the population distribution over the uniform quasicontinuum, while the number $(1 - J(x/\eta))^{-1}$ in the saddle point replaces the factor $(1 - \frac{w}{\varepsilon_0})^{-2}$ in that expression. If the integral is not of a saddle point type, still, the integration gives another, more involved population distribution profile different from that of Eq.(26).

The result obtained gives us a population distribution over an inhomogeneous quasicontinuum, which attains at times longer relative to the typical time required for a Rabi transition to an isolated level of the band. This requirement implied by the assumption that the arguments in the exponents in integrands for G and J are large, such that these coefficient are not small and indeed modify the distribution obtained earlier for the case of uniform quasicontinuum.

The physical ground of such a modification is rather transparent. Indeed, in contrast to the states surrounded by the neighboring levels from both sides, the amplitudes of state at the continuum edge do not decay exponentially. We have notice this already for the uniform quasicontinuum, – the states at the edge were responsible for the $1/t \log t$ time behavior Eq.(25) of the population. Recurrences of the population from the inhomogeneous band to the isolated level are further redirected to quasicontinuum and keep "feeding" these very slowly decaying states, in such a way that they finally form at the edge a different stationary population distribution.

The structure of the function F depends on the statistics of the matrix elements, and it may give rise to various dynamic behavior, similar to that demonstrated for the infinite quasicontinuum[5]. In the next Section we focus on one of the simplest, tractable, case, which still illus-

trates the main phenomena associated with recurrences of the population from the band to the isolated level – forming of a stationary distribution different from that of the homogeneous quasicontinuum.

X. AN ANALYTICALLY TRACTABLE EXAMPLE.

We consider an example where the distribution $g(V)$ of the level's coupling has nonzero the second $w = \int g(V) V^2 dV$ and the fourth $u = \int g(V) V^4 dV$ moments, while all higher moments are ignored. This model does not look very realistic for the case of multiphoton transitions in ensembles of interacting Rydberg atoms, where the distribution rather has a form $g(V) \propto V^{\alpha+\beta \log V}$, but still it allows one to immediately find an explicit expression for F . Apart from the contributions of the order w that have been considered for the case of the homogeneous band, it suggests three more terms, emerging from the second order Taylor expansion in Eq.(44):

$$\begin{aligned} \Delta F &= u \int_0^{\infty} dE \left(\frac{i\theta}{\xi - E} - \frac{i\tau}{\varepsilon - E} \right)^2 \\ &= -u \frac{\theta^2}{\xi} - u \frac{\tau^2}{\varepsilon} - u 2\theta\tau \frac{\log(-\varepsilon) - \log(-\xi)}{\xi - \varepsilon}. \end{aligned}$$

We have to take into account that for positive ε and ξ , the logarithms have imaginary contributions $i\pi$ for ε and $-i\pi$ for ξ , since the integration contours of the inverse Fourier transformations for these variables are above and below the real axis, respectively. The saddle point calculation of the integral Eq.(43) over $d\tau d\theta$ for the average density yields

$$\langle \rho_n(t) \rangle = \int_{-\infty+i0}^{\infty+i0} d\varepsilon \int_{-\infty-i0}^{\infty-i0} d\xi \frac{V_n^2 e^{-i(\varepsilon-\xi)t}}{(\varepsilon - E_n)(\xi - E_n)} \frac{2\pi e^{\Phi}}{D}$$

with an explicit but cumbersome expression Φ in the exponent. We only employ the zero and first order expansions for this quantity in $\zeta = \varepsilon - \xi$. In contrast, the denominator

$$D = u \sqrt{\frac{1}{\varepsilon\xi} - \left(\frac{\log(-\varepsilon) - \log(-\xi)}{\varepsilon - \xi} \right)^2},$$

emerging from the saddle point calculations, we consider explicitly and notice, that it has the Taylor expansion in ζ different for the positive and the negative η and reads:

$$\begin{aligned} D_{<} &= \frac{u\zeta}{3\eta^2} \quad \text{for } \eta < 0 \\ D_{>} &= \frac{4u\pi}{\zeta} \quad \text{for } \eta > 0. \end{aligned}$$

The explicit expressions for the exponents read

$$\Phi_{<} = \frac{\eta (7\eta^2 + \bar{E}_o^2 - 5\bar{E}_o\eta + 3w^2 - 3\bar{E}_ow + 9\eta w)}{u} + \frac{\eta w^2 \log^2(-\eta)}{u} + \frac{\eta w \log(-\eta)(-2\bar{E}_o + 5\eta + 3w)}{u}$$

and

$$\Phi_{>} = -\frac{i\zeta (\pi^2 w^2 + (-\bar{E}_o + \eta + w \log(-\eta))^2)}{4\pi u},$$

respectively.

The presence of the contribution ΔF modifies the results Eq.(26) obtained for the homogeneous quascontinuum. The second term in Eq.(23) related to the poles at the points $\varepsilon = E$ and $\xi = E$ (that is for $\eta > 0$) with the allowance of the factor $\frac{1}{D} \propto \zeta$ acquires a time dependency and disappears as $1/t^2$ with the time elapse. In contrast, for $\eta < 0$, the contribution of the pole $\frac{1}{D} \propto \zeta^{-1}$ gives rise to a new stationary profile

$$\langle \rho_E \rangle = \int_{-\infty}^0 \frac{d\eta}{u} \frac{3\eta^2 6\pi e^{\Phi_{<}}}{(\eta - E)^2}.$$

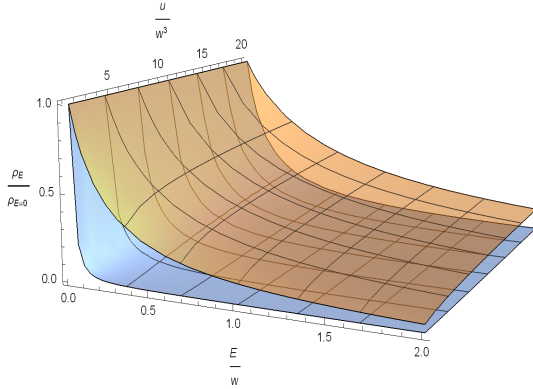


FIG. 19: Intermediate asymptotic regime allowing for the recurrences of the population from the quascontinuum back to the isolated initially populated level. Population distributions normalized to their values at the continuum edge as functions of the energy position E/w and the fourth moment of the matrix elements distribution u/w^3 for two sizes of the energy gap between the isolated level and the quascontinuum edge. The upper surface corresponds to $E_o/w = 1$, and the lower one – to $E_o/w = 10$.

In Figs.19-21 we depict the profiles of the population distribution at the quascontinuum edge suggested by this expression. In Fig.19 one sees, that the population distribution profile gets broader with the fourth moment u increasing, but gets narrower with the increase of the energy gap between the level and the quascontinuum

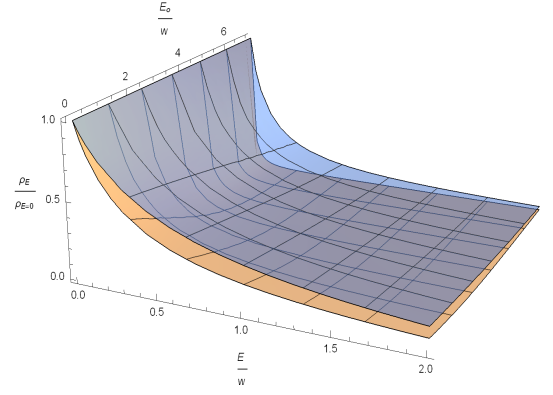


FIG. 20: Population distributions normalized to their values at the continuum edge as functions of the energy position E/w and the energy distance E_o/w between the isolated level and the quascontinuum edge for two sizes of the fourth moment of the matrix elements distribution $u/w^3 = 1$ (the lower surface) and $u/w^3 = 10$ (the upper surface).

band edge, as it is seen in Fig.20. The last trend is opposite to the case of the homogeneous band.

In Fig.21 we depict the population density at the edge as function of the gap size and the fourth moment of the coupling strength distribution.

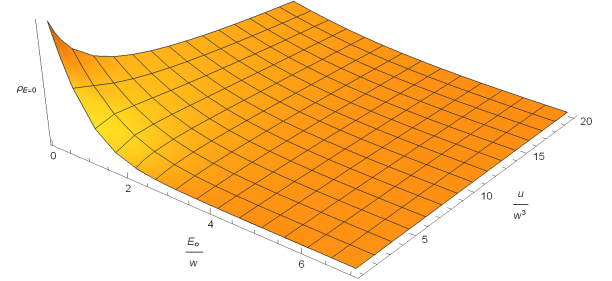


FIG. 21: Population density at the quascontinuum edge as function of the energy gap E_o/w and the fourth moment $u/w^3 = 1$ of the spoiler state strength distribution. The absolute value of this quantity obtained within the saddle point approximation cannot be considered as reliable and therefore is not given numerically in the plot.

Note that the analytically tractable case under consideration should not be taken as a reliable prediction for the intermediate asymptotic profiles. It just shows the mechanism of the modification of the population distribution due to the recurrences from the inhomogeneous quascontinuum. For the toy example just considered, the positions of the reference points η of the inverse square energy distribution $(\eta - E)^{-2}$ have a rather broad distribution dictated by the function $\Phi_{<}$ emerging for this model.

XI. NON-ADIABATIC TRANSITION TO THE EDGE IN THE PRESENCE OF NUMEROUS SPOILERS.

A natural question arises – how does the presence of numerous spoilers affect the non-adiabatic transitions to the quasicontinuum from an isolated level slowly moving toward it's edge and back? Equivalence of the non-adiabatic transition problem and the scattering problem discussed in Sec.V suggests to think about the problem of conductance and scattering by disordered media that are well-studied in the Condensed Matter Physics [16] with the help of the random matrix technique, which can also be extended to the case of the absorbing media [17].

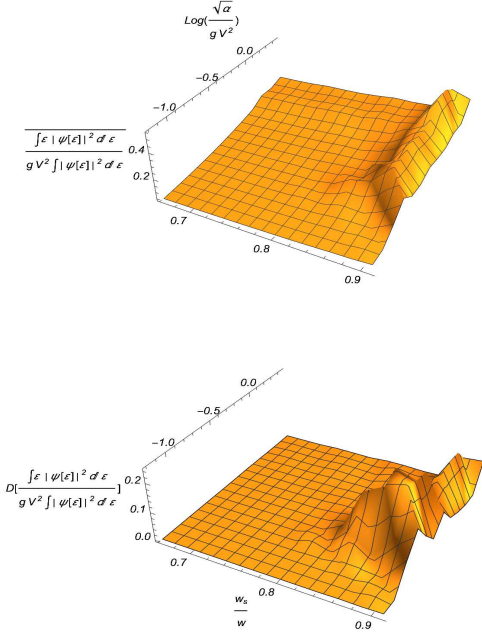


FIG. 22: Width of the population distribution in the presence of the random spoilers as function of the approach rate parameter α and the total "cross-section" fraction $\langle g_s V_s^2 \rangle / w$ of the spoiler states. In the upper plot we present the result of averaging over 50 realization each for random positions of the spoilers that are uniformly distributed over the band and over the couplings $V_s \in \{0, 10V\}$. In the lower plot we depict the dispersion of the width.

Technically, expressions for the states amplitudes Eq.(5) can be generalized on the case of slowly moving level, – in the Fourier representation they adopt the op-

erator form:

$$\begin{aligned}\psi_0(\varepsilon) &= \frac{e^{-i\varepsilon t}}{\varepsilon - E_0 - \alpha \frac{\partial^2}{\partial \varepsilon^2} - \sum_{m=1}^M \frac{V_m^2}{\varepsilon - E_m}} \psi_{t=-\infty}, \\ \psi_n(\varepsilon) &= \frac{V_n^2}{(\varepsilon - E_n)} \psi_0(\varepsilon), \\ \psi_{t=-\infty} &= \lim_{t_0 \rightarrow \infty, \beta \rightarrow 0} \sqrt{\frac{\beta}{\pi}} \int e^{-i\varepsilon t - i\alpha(t-t_0)^3/3 - \beta(t-t_0)^2} d\varepsilon,\end{aligned}$$

whence expressions for the population following from their formal solution given in terms functional integrals over some field variables are supposed to be averaged over the statistical distribution of the band levels. The resulting formal expression can be written explicitly. It contains functional analogs of the average Eq.(44)

$$F = \int dE dV g(V) \left(e^{\frac{i\theta(\xi)V^2}{\xi-E} - \frac{i\tau(\varepsilon)V^2}{\varepsilon-E}} - 1 \right), \quad (47)$$

with $\theta(\xi), \tau(\varepsilon)$ expressed in terms of the field variables employed.

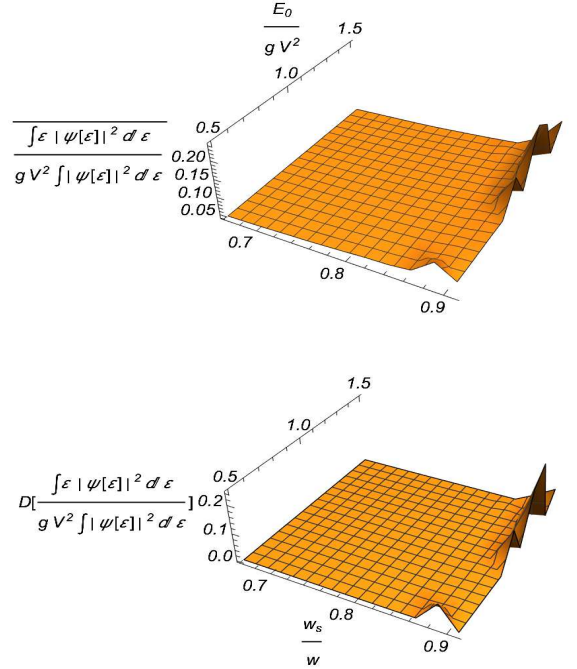


FIG. 23: Width of the population distribution in the presence of the random spoilers as function of the maximum level energy E_0 and the total "cross-section" fraction $\langle g_s V_s^2 \rangle / w$ of the spoiler states. In the upper plot we present the result of averaging over 50 realization each for random positions of the spoilers that are uniformly distributed over the band and over the couplings $V_s \in \{0, 10V\}$. In the lower plot we depict the dispersion of the width found numerically for the realizations.

However, unfortunately, the case under consideration does not fit well to the models of Gaussian random potentials usually employed for description of the disordered

media that allows one to obtain explicit formula. The non-adiabatic regime of "heavy particle", which corresponds to the optimum efficiency of the edge population, is strongly affected by the "classically allowed" domains of the "scattering potentials", incompatible with the model of uncorrelated potentials implied by Gaussian statistics. We therefore leave the analytical approach to the problem for future research, and here we just present results of the numerical calculations performed for different random realization of the spoiler position and strengths, each of which gives a specific population distribution, and these distributions are averaged over the ensemble of 50 random realizations. In order to check whether or not the averaging is meaningful, we perform averaging three times, over three sets of 50 randomly generated realizations each.

In Figs.22 and 23 we present the results of these calculations. One sees, that the distribution remains rather well localized at the continuum edge. Still, from the dispersion of the dependencies shown in the lower plots of each figure, one sees that the population distribution width turns out to be rather sensitive to the particular realization of the spoiler position and couplings in the regime of slow motion and in the regime of large "penetration energy" E_0 of the level to the band. Presumably, this indicates, that the main "spoiling" effect rather comes from a single, the strongest, spoiler or from a few of the most strong of them.

XII. SUMMARY OF THE RESULTS OF THE LEVEL-BAND EDGE DYNAMICS.

We summarize the results of the consideration of the population dynamics of the quasicontinuum – a dense band of states located in the positive part of the energy axis E with the edge at the point $E = 0$. For the uniform quasicontinuum, for the population transferred from an isolated level with the negative energy after an abrupt switch on of the interaction, a stationary distribution attains, which consists of two similar parts. Each of the part can be seen as a "tail" of a $1/(E - E_s)^2$ distribution, which extends to the domain of positive energies, with the reference energies $E_s = E_1$ and $E_s = 0$ located at the negative part of the energy axes. Position of the reference levels are different, – one is close to the position of the isolated level, which is just displaced by the Stark effect due to the interaction with the quasicontinuum, while the other locates closer to the continuum edge and is given by the Lambert function. This stationary distribution attains with the time dependence $(t \log t)^{-1}$.

If the continuum is not uniform and contains "spoiler states" – a number of strongly coupled states locating in the quasicontinuum, the distribution gets transformed. Each of the spoiler state, takes a certain amount of the population and redistributes it among the other, weak, states of the quasicontinuum that are close in energy to the spoiler. The distribution near the edge does not ex-

perience a big change of its shape, but just loses a part of its total population.

If the spoilers are numerous and randomly distributed in their energies and in their coupling strengths, the overall distribution still remains localized near the quasicontinuum edge, but the distribution profile may experience a change of its shape, dictated by the statistics of the spoiler strengths. Also the time law, with which the distribution attains experience a variation. This reflects the role of the interplay of the process of population recurrences back to the isolated level from the nonuniform quasicontinuum and the process further redirection of this populations to the band. The resulting distribution is a convolution of the inverse square dependence $1/(E - E_s)^2$ and the distribution of the reference energy position E_s specific for the statistics of the spoiler strength $g(V)$.

The energy distribution of the population over the band states gets much narrower for the case of the isolated level slowly approaching the band edge and returning back according the law $E_0 - \alpha t^2$. The non-adiabatic transfer of the population to the continuum edge is controlled in a crucial way by the scaled rate $\alpha/(gV^2)^2$ of the level's parabolic approach. The population profile roughly corresponds to the dependence $\alpha/(gV^2)$ of the width on these parameters, which directly relates to the time-energy uncertainty principle.

Presence of the spoiler states also affect this distribution, but in much weaker way, compared to the case of the abrupt switch on of the interaction.

XIII. DISCUSSION OF THE RESULTS IN THE CONTEXT OF QUANTUM COMPUTATIONS.

We now discuss meaning of the results obtained for the strategy of quantum computations. We stay in the paradigm, that the quantum algorithms are physically realized as multiphoton Raman transitions from the well defined initial state to a narrow strip of the quantum states located near the lowest edge of the spectrum of the corresponding Hamiltonians, and imply technically just a set of simple manipulations such as tuning of the external fields to required frequencies keeping coherence of the system during a sufficiently long period along with a proper choice of the strengths of the interactions and, if necessary, a slow variation of these parameters.

One may also want to define a parameter that can somehow characterize "complexity" of quantum algorithms in the context of Raman excitation. Traditional measure of complexity, that is the number of operations required for achieving the computational goal, cannot be employed, since the Raman excitation approach does not require a big number of operations. We therefore propose to characterize the algorithms by the product a typical number of the populated levels after the excitation procedure and a typical time required for the corresponding distribution to attain. For the Grover's algorithm, this parameter equals to the time of a single operation multi-

plied by the square root of the Hilbert space dimension. In contrast, for all algorithms based on the excitation of the quasicontinuum edge, this parameter is of the order of the Heisenberg return time $\sim \hbar g$. In fact, for the case discussed in Sec.IV, the typical time when distribution Eq.(26) attains is of the order of $\hbar/w \sim \hbar/V^2 g$, while the typical distribution width parameter w implies that the number of the populated levels is of the order of wg . Same is valid for the case of Sec.V, where the typical distribution width is of the order of $\sqrt{w/\alpha}$, the typical number of the populated states is therefore $\sqrt{w/\alpha}g$, while the typical time t_{typ} of the excitation process emerging from the condition $\alpha t_{typ}^2 \sim w$ also yield the same estimate of the parameter.

If one considers the process of population of just one, presumably the lowest, state in the band, the required time simply equals the inverse gap - the distance between the lowest and the second lowest levels. This is completely consistent with the uncertainty principle. Of course, the same estimate remains also valid for the Grover's algorithm when the lowest state is separated from its nearest neighboring state by a gap of a finite size. In other words, the time-energy uncertainty principle is the only physical restriction of the algorithm efficiency, - the algorithms realized as the Raman excitation of the uniform quasicontinuum thus differ not by the efficiency parameter but just by the "form-factor" governing the shape of the population distribution near the edge.

The efficiency of the algorithm apparently gets worth in the presence of the spoiler states. For an unknown structure of the distribution of the Raman couplings over the spectrum, realization may require an optimization procedure, that is aimed to diminish the influence of the role of "spoilers". This means, that the excitation of the atomic ensemble has to be performed several times in order to sequentially identify position of the spoilers strongly affecting the population distribution, and adjusting the excitation parameters in a way excluding this influence. The strategy in question should, in our opinion, be the following. One starts by estimating the average value of the interaction and the state density. Next one performs a series of excitations and experimentally measure the populated energy eigenstates and finds the corresponding energies. If the identified energies are far from the edge, one can guess, that the role of the "spoiler" states is dominating, and therefore the size of the interaction (or the detuning change velocity) has to be reduced. This has to be done a number of times until the population of "spoilers" became unlikely. Non-adiabatic algorithm seems to be more suitable for such a strategy. In some sense, such a procedure is an analog of that performed in the approach of Ref.[8], where the parameters of the excitation protocol subject to variation in function

of the atomic ensemble average energy measurement.

XIV. CONCLUSION

We conclude by summarizing the concept of Quantum Algorithms seen as a Raman excitation of an ensemble of Rydberg Atoms. Quantum computation implies transition from a well-defined initial quantum state of an ensemble of two-level systems to the target quantum state of a well-defined energy position and initially unknown state vector given in the computational basis, that is terms of binary occupation numbers of the two-level registers, whence measurement of the register states yield the required result of the computation. The process also implies existence of the hardware and the software. In the context of ensemble of Rydberg atoms, the software is seen as an interatomic interaction Hamiltonian diagonal in the computational basis and an interaction Hamiltonian controlled by external laser fields, while the target state corresponds to the edge of the spectrum. Exact calculation means complete transfer of the population to the target state at the edge, while the approximate calculation, in this context, mean transfer of the population to a group of states close to the edge.

In other words, in the framework of such a concept, Quantum Algorithms are seen as controlled processes of the population dynamics near the spectrum edge, where the accuracy of the approximation turns to be limited by the time-energy uncertainty principle exclusively. The number of the populated levels multiplied by the time required for the population remains of the order of the Heisenberg time given by the quantum state energy density near the edge, which in the extreme of the single populated level is of the order of the inverse energy gap between the edge level and its nearest neighbor. Various population strategies differ only by a form-factor related to the shape of the population distribution profiles.

Still, there is an important complication in achieving the uncertainty relation limit caused by eventual heterogeneity of the band level couplings, which we call the presence of "spoiler states" - strongly coupled levels located rather far from the edge. In order to avoid influence of these states, the excitation procedure has to be performed in several steps, each of which is supposed to identify by measurement the spoiler states close to the edge at a given strength of the Raman coupling followed by decreasing of the coupling strength in accordance with the measured spoiler energy position in order to eliminate its population. Sequential application of such identification and elimination with decreasing Raman coupling strength allows one to approach the states at the spectrum edge.

[1] E. Fermi, *Notes on Quantum Mechanics*, Sec. 23, (University of Chicago Press, 1960).

[2] M. Bixon and J. Jortner, *Intramolecular radiationless*

- transitions, J. Chem. Phys. 48, 715 (1968)
- [3] U. Fano, *Effects of configuration interaction on intensities and phase shifts*, Phys. Rev. 124, 1866 (1961).
 - [4] Yu. N. Demkov and V. I. Osherov, *Stationary and non-stationary problems in quantum mechanics that can be solved by means of contour integration*, Sov. Phys. JETP, 26, 916 (1968).
 - [5] V. M. Akulin, *Dynamics of Complex Quantum Systems*, (Springer, New York, 2014).
 - [6] E. Farhi, J. Goldstone, S. Gutmann, J. Lapan, A. Lundgren, and D. Preda, *A Quantum Adiabatic Evolution Algorithm Applied to Random Instances of an NP-Complete Problem*, Science 292, Issue 5516, 472 (2001); E. Farhi, J. Goldstone, S. Gutmann, and M. Sipser, *Quantum Computation by Adiabatic Evolution*, arXiv:quant-ph/0001106 (2000).
 - [7] T. Albash, and D. A. Lidar, *Adiabatic Quantum Computing*, Rev. Mod. Phys. 90, 015002 (2018).
 - [8] E. Farhi, J. Goldstone and S. Gutmann, *A Quantum Approximate Optimization Algorithm*, arXiv:1411.4028 (2014).
 - [9] S. Ebadi et al, *Quantum Optimization of Maximum Independent Set using Rydberg Atom Arrays*, arXiv:2202.09372v1 (2022).
 - [10] M. D. Lukin, M. Fleischhauer, R. Cote, L. M. Duan, D. Jaksch, J. I. Cirac, and P. Zoller, *Dipole Blockade and Quantum Information Processing in Mesoscopic Atomic Ensembles*, Phys. Rev. Lett. 87, 037901 (2001).
 - [11] I. Mourachko, D. Comparat, F. de Tomasi, A. Fioretti, P. Nosbaum, V.M. Akulin, and P. Pillet, *Many-body effects in a frozen Rydberg gas*, Phys. Rev. Lett. 80, 253 (1998).
 - [12] L. Grover, In Proc. 28th Annual ACM Symposium on the Theory of Computation, pages 212-219, ACM Press, New York, 1996; L. K. Grover, *Quantum mechanics helps in searching for a needle in a haystack*, Phys. Rev. Lett. 79, 325 (1997).
 - [13] A. Browaeys, and T. Lahaye, *Many-body physics with individually controlled Rydberg atoms*, Nat. Phys. 16, 132-142 (2020).
 - [14] A. Glaetzle, R. van Bijnen, P. Zoller, et al., *A coherent quantum annealer with Rydberg atoms*, Nat Commun. 8, 15813 (2017).
 - [15] H. Pichler, S.-T. Wang, L. Zhou, S. Choi, and M. D. Lukin, *Quantum Optimization for Maximum Independent Set Using Rydberg Atom Arrays*, arXiv:1808.10816 (2018).
 - [16] K. Efetov, *Supersymmetry in Disorder and Chaos*, (Cambridge University Press, New-York, 1997).
 - [17] S. B. Fedeli, Y. V. Fyodorov, *Statistics of off-diagonal entries of Wigner K-matrix for chaotic wave systems with absorption*, J. Phys. A 53, 165701 (2020).